



Mathematisch-Naturwissenschaftliche Fakultät
Ernst-Moritz-Arndt-Universität Greifswald

Bachelor Thesis

Sand and snow dunes with cellular automata

Tim Teichmann
Greifswald, July 9, 2010

Gutachter:
Prof. Dr. Ralf Schneider
PD Dr. Berndt Bruhn

Contents

1	Motivation	3
2	Theoretical background	4
2.1	Dynamics in sand piles	4
2.2	Behavior of blown sand on small scales	5
2.3	Structure formation	6
2.4	Dune shapes	6
2.5	Dynamics of dunes	7
2.6	Cellular automata	7
3	Basic algorithm	9
3.1	Erosion	9
3.2	Transport	9
3.3	Sliding	10
4	Results	11
4.1	Building up a sand pile	11
4.2	Testing different erosion / transport rules	13
4.3	Structure formation	13
4.3.1	From a flat surface	13
4.3.2	From a small transverse dune	14
4.4	Movement and stability	15
4.5	Parameter variations	17
4.5.1	Transport length	17
4.5.2	Erosion rate	20
4.5.3	Total amount of sand	21
4.6	Correlation of dune size and dune velocity	23
5	Conclusions and outlook	24
	Bibliography	26

1 Motivation

One of the remaining challenges for physics in this century is a better understanding of turbulent systems. The route from order to chaos and the creation of structures in turbulence is one aspect of common interest in this field connecting so different fields like meteorology, fusion plasmas and fluid dynamics. An example for structure creation in turbulence is the situation when turbulent wind in clouds leads to the collision of small water droplets merging into larger drops, which can be seen as rain [1]. Another example is the turbulent deposition and transport of sand under the influence of wind in deserts, forming sometimes dunes.

One approach to simulate large and complex systems is the concept of cellular automata, where the complicated dynamics of the system are reduced to a small set of simple rules.

The aim of this thesis is to develop a model to simulate the creation and temporal evolution of dunes using a cellular automaton and to qualify and validate it. Therefore first some background information about dynamics in sand piles, the interaction between wind and sand, dune shapes and formation and cellular automata is given in section 2. Then in section 3 the rules for the cellular automaton are discussed. In section 4 the results are discussed, beginning with a comparison of different rule sets, that would have been possible to use, followed by observations of structural changes in a dune field and an analysis of how changes of parameters (such as the velocity of sand transport) affect the properties of a dune field. Finally it is tested, whether the functional relation between size and velocity of a dune. The results are summarized in section 5.



Fig. 1.1: *A field of barchan dunes photographed from an airplane.*

2 Theoretical background

2.1 Dynamics in sand piles

Understanding the dynamics in sand piles is of great interest, because they are a relatively simple example of self-organized criticality (SOC) and can therefore be used as a model system for other processes with SOC behavior, such as earthquakes [2], cloud creation [3], evolution of population [4], forest fires [5] and edge effects in tokamaks [6]. The concept of SOC was introduced by Bak, Tang and Wiesenfeld [7,8] and states, that an open, driven system strives towards a “critical” state, which is locally unstable and has no intrinsic time or length scale.

Such systems show three characteristics, which are often observed in nature. The first one is fractal structure: The systems look the same independently from the length scale (this is the case in turbulent winds). The second one is $1/f$ -noise: The energy of occurring noise rises with the decline of its frequency (which is the case for example in resistors). The third one is the power law: An event is more likely to happen, when its effects are smaller in some sense, in a way that a log-log-diagram of event size and frequency would give a straight line (as it is the case for the occurrence of earth quakes).



Fig. 2.1: *The size distribution of clouds can be described by a power law. Furthermore the processes in them can be described by self organized criticality.*

Large amounts of sand grains – as well as snow flakes in powder snow – can be approximated as spherical particles. If too many of those particles are put onto the same area the upper ones will slide down and a pile is formed. The angle at which such a sand pile is still stationary (but unstable) is called “angle of repose”. According to Mehta and Barker [9] there is a range of angles of repose, because a smaller angle of repose is needed to keep a movement continuing than to initiate it.

Within this range any sand pile can be in a stationary as well as in a sliding condition. The interval of angles of repose is limited by the maximum angle at which a stationary sand pile will begin sliding as soon as any more sand is added – the “maximum angle of stability” α_m – and the angle at which it ceases to slide – the “minimal angle of repose” α_r . According to Bagnold [10] the angle of repose depends mainly on the shape and size distributions of the particles. $\alpha_m = 34^\circ$ and $\alpha_r = 30^\circ$ are reasonable values for sand.

Mehta and Barker assume, that an avalanche starting in one direction will exist until the minimal angle of repose is reached in this direction, while other models (for example by Alonso and Herrmann [11]) include the momentum of the particles in the condition for the avalanche to stop, which allows tails at the bottom of sand piles.

2.2 Behavior of blown sand on small scales

As soon as wind faster than a certain threshold velocity streams over a patch of sand, some of the grains will begin to move. Bagnold classifies this movement of sand grains into three groups: suspension, saltation and surface creep [10].

Suspended sand grains are usually very small and therefore light. They are transported with the stream and can travel rather long distances, because collisions with particles coming from below compensate the gravitational force.

Saltated grains are usually medium sized. They were ejected by the momentum a landing grain transmitted to them. Their vertical velocity behaves just like that of a thrown object (with friction), but as the particle is slowed down relative to the wind it is accelerated relative to the bottom until it reaches approximately wind velocity. This kind of transport becomes rather dominant when the grain size varies strongly, because heavier particles can launch smaller particles with higher velocities.

The third kind of movement is the surface creep. Since the landing particles have quite a small angle of impact, the biggest part of its energy will be transmitted in a direction parallel to the wind. This leads to creeping forward especially for larger grains because they are pushed by a large number of other particles which were in saltation or crept before.

Following Bagnold, the total sand flow is given by

$$q = C \cdot \sqrt{\frac{d}{D}} \cdot \frac{\rho}{g} \cdot v_*^3$$

It depends on the velocity gradient of the wind v_*^3 , the mean diameter of the sand grains (divided by a normalization parameter of 0.25 mm) $\frac{d}{D}$ and a constant C depending on

the size distribution amongst the grains as well as on the mass density ρ of air and the gravitational acceleration g .

2.3 Structure formation

Once the sand is moving, sooner or later small local instabilities of sand height will arise, because of the statistical characteristics of sand transport. Accumulations that formed this way have a slope in wind direction which is positive on one (defined to be the windward) and negative on the other (the leeward) side. Since the component of the velocity of saltated grains parallel to the wind is quite high at landing time, their angle of impact is very low. This means, that it is far more likely, that a saltated grain lands on the windward than on the leeward side. Therefore, the accumulation increases and first ripples are formed.

2.4 Dune shapes

For different geographic conditions – such as strength and direction of wind or amount of sand supply – different types of dunes emerge [10,12,13]. Some of the most important types are:

- **Transverse dunes**, which are very long ridges, oriented perpendicular to the wind direction. They build up, when the wind blows unidirectional, especially when there is so much sand available, that the bottom (consisting of larger pebbles) is always covered with sand.
- **Barchan dunes**, which are crescent-shaped dunes, opened downwind. They develop, if the wind blows from only one direction over a certain time and when not too much sand is available. Barchans move parallel to wind direction and can sustain their shape for very long times.
- **Seif dunes**, which are sinus shaped linear dunes, oriented parallel to the main direction of the wind. They can only build up if the wind blows from multiple directions. The standard picture for their creation is that one arm of an existing barchan dune is blown away by a weaker crosswind, forming a small diagonal dune. As those wind variations are linked to the seasons and therefore appear annually, the sand blown over the barchan will feed the new diagonal dune and it will become larger than the barchan itself over time.
- **Star dunes** (which are star shaped) and **network dunes** (which consist of overlapping transverse dunes). These are the most complex dune shapes possible. They appear when many wind directions with about equally strong winds appear periodically.

In some publications all dunes with a slip face parallel to the main direction of the wind are called **transverse** dunes (which then includes barchans and therefore all dunes covered in this thesis). Dunes with the net transport of the sand parallel to their crest are called **linear dunes**.

2.5 Dynamics of dunes

Dunes that are exposed to the wind move – even while they are formed. From practical considerations, definitions of dune velocities make sense only for dunes of constant sizes and shapes. According to Livingstone [13] the velocity of a transversely moving dune, which is not anchored by vegetation, can be calculated by

$$v_d = \frac{q_b}{kH\rho_b}$$

where q_b is the sand flux that is trapped by the dune, H is the dune height, ρ_b is the mass density of the sand (including the air between the grains) and $k = \frac{A_C}{LH}$ is a parameter consisting of the cross-sectional area A_C , the path between neighboring dunes L (which can also be seen as a wavelength) and the dune height.

Rubin and Hunter stated, that $k = 0.5$ could be assumed for simplified triangular dunes [14] and Bagnold used the total sand flux q instead of q_b and set $k = 1$ [10], which is nearly the same if half of the sand blowing over the dune is trapped. In any case k was assumed to be constant.

q_b is thought to depend mainly on the amount of sand which is trapped, when the air stream rips off over the slip face. This amount is nearly independent of the size of the dune, but depends on its shape. This means that with a constant sand flux q , q_b is constant as well, which leaves the relation

$$v_d \propto H^{-1}$$

2.6 Cellular automata

To simulate large and complex systems quite fast and efficient one possibility is to use the concept of cellular automata. A cellular automaton is characterized by the following rules [15]:

- The simulated area is divided into many cells.
- Those cells can have only a limited number of states.
- All cells are connected among themselves – for example by setting the cells onto points of a lattice.
- The state of a cell can only be influenced by cells in a limited neighborhood of the cell itself.

- The change of cell states is defined by a very limited set of rules.
- Those rules are applied in every time step of the simulation.

One of the simplest and probably best known cellular automata is “Conway’s Game of Life”. It can be seen as a model for ecological balance. The automaton consists grid of squares, each representing a population, that is either living or dead. The survival of a population depends solely on how many of its eight neighbors are living. Populations with less than two living neighbors die of loneliness, populations with more than three living neighbors die due to overcrowding. A dead population can only be revived, if it has exactly three neighbors. Whether a population will live or not in the next time steps is determined in parallel for all cells.

The rules, that were used for the simulation of sand dunes are described in the next section.

3 Basic algorithm

In the simulation program the simulated area is divided into equally sized, squared cells. For each cell an average sand height is given. The following three steps are performed on every cell during each time step:

- Erosion
- Transport
- Sliding

The rules for those steps are inspired by papers written by Francisco de Castro [16], Hiraku Nishimori and Noriyuki Ouchi [17].

3.1 Erosion

Due to the wind a certain amount of sand is dragged into the air above every cell. In the simulation, this amount is given by a base amount E_0 , which is randomly generated within a (user defined) limit for every cell and time step and then multiplied by a function of the slope. Nishimori and Ouchi suggested $q = q_0 + b' \cdot \tanh(\nabla h)$ as a reasonable equation for this purpose, which leads to the amount of the eroded sand on a cell:

$$E = E_0 \cdot (1 + 0.9 \cdot \tanh(\nabla h))$$

In this formula ∇h is the slope in wind direction on the considered cell. It was determined by measuring the height difference between the two adjacent cells in wind direction and dividing it by twice the cell size d . The lifted sand is subtracted from the sand height on the cell and noted as sand in the air. Of course there cannot be more sand removed from any cell, than it holds.

3.2 Transport

For every cell with airborne sand a wind velocity dependent “effective transport length” L is randomly generated within borders representing the wind velocity. The lifted sand from such a cell is then transported to the neighboring, leeward cell. After this its transport length is decreased by a certain distance L_- and the transport step is repeated on the next cell. When the remaining transport length reaches zero, all sand is dropped

onto this cell.

The function

$$L_- = d \cdot (1 - \tanh(\nabla h))$$

with the cell size d and the slope of the traveled distance ∇h (determined by dividing the height difference between the current cell and the cell the sand came from by the cell size) seems suitable. It makes the sand travel longer distances when it is on the windward slope (where the wind is further pushing it) and only short distances on the leeward side (where the wind stream might be ripped of).

Since the simulations were only performed with unidirectional wind, the wind was defined to blow in x -direction.

3.3 Sliding

After the sand has been transported, it might be stacked high enough to form an unstable sand pile. It is assumed that the sand will begin to slide from a cell, when the maximum angle of stability is reached on one of the eight slopes leading away from the cell. Furthermore, it is assumed that an avalanche will start only in the direction of the steepest slope. Since the sand then strives to reach the minimum angle of repose, it seems logically, that the difference in height between the two affected cells is only dependent on the distance between the cells and the minimal angle of repose. Therefore the transferred amount of sand from cell two to cell one is calculated by

$$\begin{aligned} d \cdot \tan \alpha_r &= h_2^{\text{new}} - h_1^{\text{new}} \\ &= (h_2^{\text{old}} - h_{\text{trans}}) - (h_1^{\text{old}} + h_{\text{trans}}) \\ \implies h_{\text{trans}} &= \frac{h_2^{\text{old}} - h_1^{\text{old}} - d \cdot \tan \alpha_r}{2} \end{aligned}$$

where d is the distance between the cells.

For all cells on the grid first the steepest downward slope is chosen and then – if necessary – the amount of sand specified in the above equation is transferred between the two adjacent cells.

At the beginning of the next section it will be made plausible why these algorithms were chosen for the simulation.

4 Results

4.1 Building up a sand pile

In the model used for the dune simulation, all triggered avalanches have the same size. This is due to the following issues: The range of height differences between two cells is limited to $h_{\text{range}} = \Delta h_m - \Delta h_r = d \cdot \tan \alpha_m - d \cdot \tan \alpha_r$, when no sliding occurs. Since slides will only start if the slope between two cells is larger than α_m the transferred height is bounded below with

$$h_{\text{trans}} = \frac{h_2 - h_1 - d \cdot \tan \alpha_r}{2} \geq \frac{(h_1 + d \cdot \tan \alpha_m) - h_1 - d \cdot \tan \alpha_r}{2} = \frac{h_{\text{range}}}{2}$$

Now consider three consecutive cells (A, B and C) of a larger slope, while one avalanche affects all of them. At the moment when the avalanche already moved sand from A to B (but not yet from B to C) the height difference between A and B is Δh_r , so the height of A could still increase by h_{range} until the next slide between those cells happens. Next the avalanche moves on from B to C, decreasing the height of B by at least $\frac{h_{\text{range}}}{2}$. This means, that the amount of additional sand allowed on A without causing a slide is decreased by this amount. Since at least $h_{\text{trans}} \geq \frac{h_{\text{range}}}{2}$ will be transferred to A, as soon as the next (local) slide occurs, there must be a slide from A to B following.

Therefore with this model it is unavoidable, that every avalanche grows to the maximum possible size after each cell was involved in an avalanche at least once. To achieve a more realistic avalanche distribution it is necessary to perform slides over larger distances instead of cell by cell.

One approach to do this was presented by Prado and Olami [18]. They designed a cellular automaton, where in addition to a height representing the number of grains laying on it, each cell is given an additional state “energy”, which represents the sum of the kinetic energies of all its grains. Each time when a slide occurs, two grains are subtracted from the higher cell and one is added to on the nearest and next nearest neighbor cell (in avalanche direction). Each of those cells get their energy value increased by one (representing the transformed potential energy of the grain) plus half of the energy of the cell they came from (which gets its energy set to zero afterwards, representing energy conservation). Unlike most other models their model does not use a constant angle of repose. Instead higher amounts of energy on a cell will trigger slides at smaller height differences. The idea behind this concept is, that sand grains are more likely to change their position, when they are pushed or dragged by other grains with a high momentum. In my implementation slides occur ed, when the height difference between two cells exceeded $h_{\text{crit}} = \lceil 4.5 - 0.3 \cdot \epsilon \rceil$, where ϵ is the total energy of the higher cell and [...]

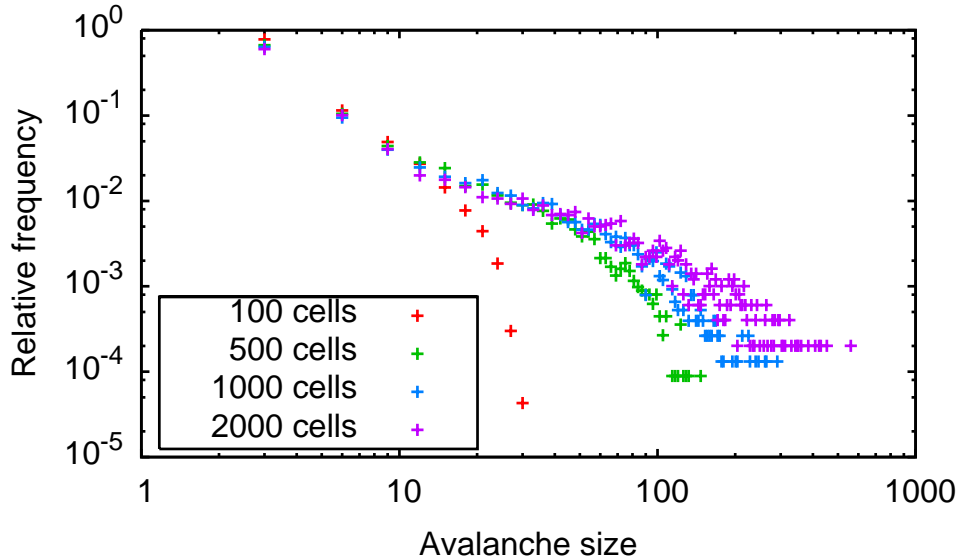


Fig. 4.1: *Relative frequency of differently sized avalanches in a sand pile modeled as proposed by Prado and Olami*

means that the value is rounded up. Furthermore $h_{\text{crit}} \geq 3$ was defined, so for $\epsilon \geq 5$ $h_{\text{crit}} = 3$ is used.

Using this model an experiment conducted by Held et al. [19] was simulated. They mounted a circular disk onto a scale and added sand onto the middle of it grain by grain. Once a sand pile reaching to the edge was built up (and sand begins to fall from the disc), the size of an avalanche reaching the edge can be determined by measuring the mass difference each time after putting a grain on top. This experiment was repeated by Naoto Yoshioka [2], who focussed on comparing how the avalanche size distributions change with varying disc and grain diameters.

In Fig. 4.1 the distributions for different numbers of cells can be seen. Small avalanches dominate the total number of avalanches by far. The differing curves for different numbers of cells (which correspond to different disc diameters) concur with the experimental result published in Yoshioka's paper for disc which are not too large.

However this model is quite time consuming even in a one-dimensional simulation. Furthermore it is nicer to have the possibility to use real numbers from the beginning. This is why the de Castro's sliding model is used instead Prado's. It is much faster converging towards a stable state (especially very fast for small height changes).

The fact that de Castro's model is not realistic considering avalanche dynamics in a sand pile, is not a big problem, because the important thing when simulating dunes using a cellular automaton is to keep the slopes within the angles of repose. The details of how they slide there are not that important.

4.2 Testing different erosion / transport rules

To find out which rule set is the best to simulate a field of dunes, combinations of the following rules were tested on an one-dimensional stripe with constant initial height.

Erosion rules:

- The amount of sand eroded on a cell is not at all dependent on the topography.
- Same, but no sand is eroded, when the cell considered is inside a lee-zone behind a dune. This zone begins behind every crest and ends as soon as a line between surface and crest has a slope of less than determined by a certain angle of shelter.
- The amount of eroded sand depends on the slope at the considered cell ($E = E_0 (1 + C \cdot \tanh \nabla h)$).

Transport rules:

- The transport length is decreased by the same length on every cell.
- The transport length is decreased by the length traveled parallel to the surface.
- The transport length is decreased by $L_- = L_{-0} (1 + C \cdot \tanh \nabla h)$

Using the topography independent erosion rule, structures could only be found using the last transport rule. When using either the approach including the lee-zone or the tanh-approach for erosion, all transport rules developed structures.

The concept of having wind shelter on the leeward side of the dune has the disadvantage, that no sand at all is eroded on long slopes with an angle slightly under the shelter angle (while in reality the wind regime would probably be restored after some distance). The concept of making the amount of eroded sand dependent on the slope seems more promising. It is a better approximation to the observation made by Bagnold, that more sand is eroded on the windward up slope than on the leeward down slope and that this effect gets even larger with steeper slopes.

Therefore, the “tanh” rules seem to be the best choice, for both the erosion and the transport step.

4.3 Structure formation

4.3.1 From a flat surface

Most of the simulations have been initialized with a flat sand sheet of constant height. Since the amount of eroded sand and the transport length vary between cells and in time, small sand piles will form by chance on random spots of the map. Because the windward slope makes the transported sand lose energy and because sand may just get stuck on the slope, more and more sand accumulates near those spots.

If the result of this process is assumed to be a sand pile, the slope on every side is the same, but the slope in wind direction is larger in the middle of the dune and smaller where the cross section in wind direction is smaller. This and the fact, that the up slope is shorter near the edge, lead to a faster progression of sand situated there, which leads to the formation of barchans. Of course, this is also true for any other formation mechanism with the exception of transverse dunes, because they are so widespread, that they have no edge in wind direction.

4.3.2 From a small transverse dune

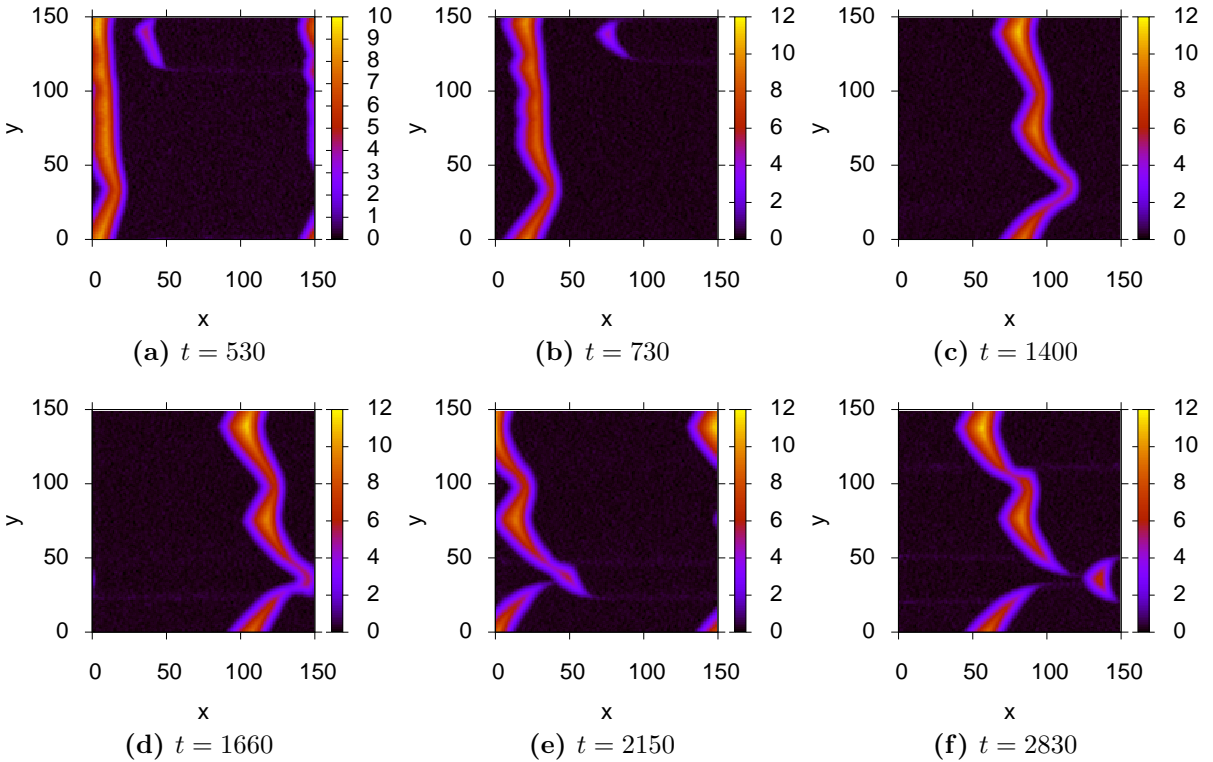


Fig. 4.2: Height maps for several time steps of the same simulation. A single (stable) transverse dune was separated from a dune field and its bottom was cut off to accelerate the transformation. One can see, that the dune is torn apart at about $y = 35$, because it is smaller and therefore faster.

Once formed, transverse dunes are usually stable. Due to the statistical characteristics of the system at any time more than the average amount of sand could be lost in a small segment of the crest. This leads to the same edge effects described earlier in section 4.3.1, however due to the slope of the slip face the wings of a potential barchan would be carried away even faster, which means the only thing left is a notch in the crest.

Smaller dunes need less sand to be rearranged when moving. The same thing is true for sections of lower height in transverse dunes. Because of this, the section with the notch will proceed faster than the rest of the dune, giving it a curved crest. There is the chance, that neighboring parts of the dune will lose height, too, or that enough sand is accumulated on the runaway section to slow it down. If neither of these options happens, the transverse dune will be torn apart sooner or later. This can be seen in Fig. 4.2.

On high transverse dunes this process happens very slowly, because a lot more sand needs to be removed to change the height of the crest by the same amount and the same height difference has a smaller impact on the dune velocity for higher dunes.

To make it easier to compare results within this thesis, all values used in figures are gained with the same set of initial parameters (except the ones specified near the figures):

- The cell size is $d = 1$.
- The angles of repose lie between $\alpha_r = 30^\circ$ and $\alpha_m = 34^\circ$.
- The erosion rate is generated between $X_{\min} = 0.16$ and $X_{\max} = 0.20$.
- The initial transport length is generated between $L_{\min} = 3$ and $L_{\max} = 6$.

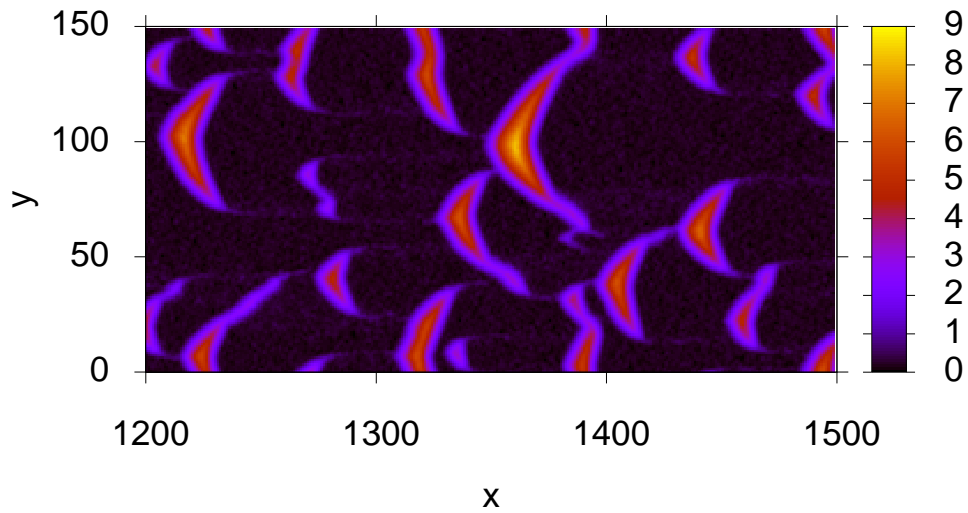
4.4 Movement and stability

If the height profiles of all time steps are retained, they can be sliced into two-dimensional height profiles with constant x - or y -coordinates. Those slices can later be reassembled to visualize the temporal development of a stripe within the simulated area.

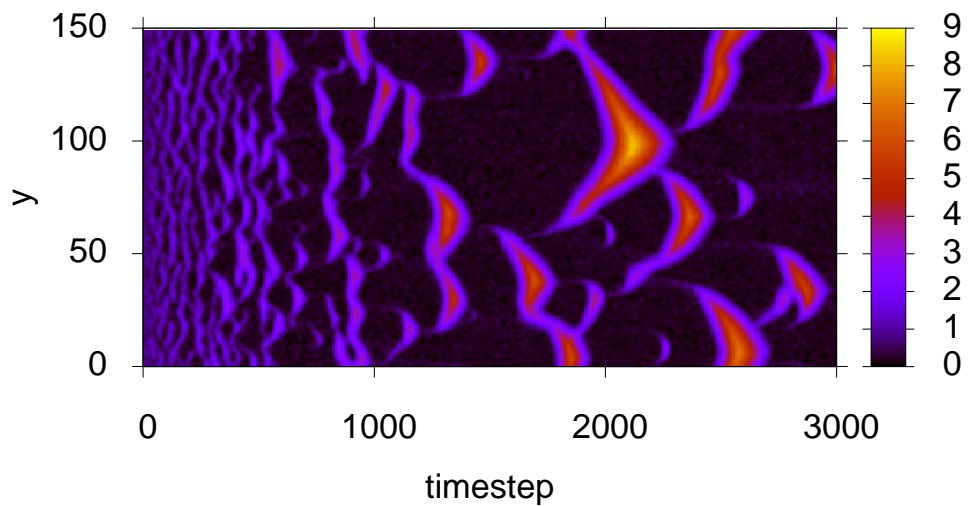
In Fig. 4.3(a) the height map of a selected area at time step $t = 2130$ is presented. Fig. 4.3(b) shows the heights at $x = 1360$ for different time steps. Notice, that the abscissa shows the temporal development instead of the x -position there. Comparing these two figures, it can be seen that the right parts of the images seem to be mirrored. This is the case, because the dunes keep their shape and while passing the cutting stripe the same forms are “scanned”. The dunes are mirrored, because the parts passing the line first are right on the height map (because they can then pass the line earlier), but left on the t - y -plot (because the moment of passing is a longer time ago for them). On the left part of the figure the formation of first small ripples and then barchans of growing size can be seen.

In Fig. 4.4 slices with constant $y = 119$ at different times are shown. Since the dunes do not move in y -direction, the history of single dunes can be followed as lines. The slope of such a line indicates the inverse velocity of the dune and its color represents the height of a certain point on the dune at a certain time.

The small dunes seen on the left edge of Fig. 4.3(b) can be seen as very short lines at the bottom of Fig. 4.4. Only few of these dunes grow and survive. In the rest of the plot it can be seen, that some dunes are not sufficiently supplied with sand and become



(a) Height map



(b) x -slice

Fig. 4.3: Fig. (a) shows the height map of a simulated area at time step $t = 2130$. Fig. (b) shows the temporal development of a slice at $x = 1360$ for the same run.

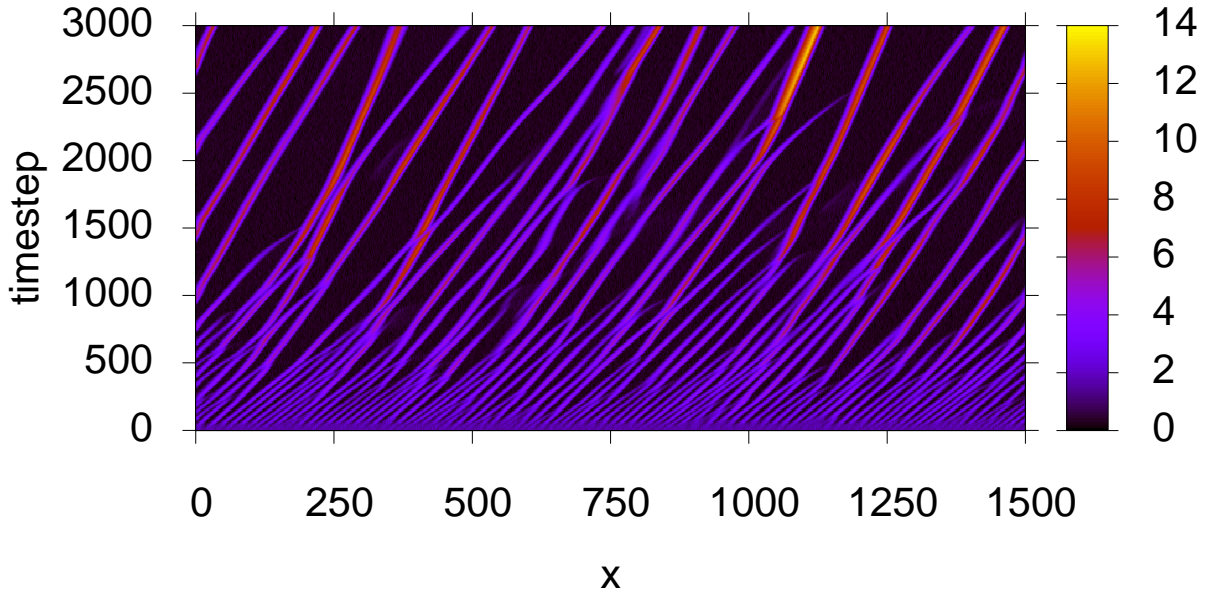


Fig. 4.4: *Horizontal stripes correspond to a slice of the simulated dune field at $y = 119$ at a given time. The lower stripes correspond to earlier time steps. The color shows the height level of a given cell at a given time. The diagonal lines can therefore characterize the movement of a dune.*

smaller and faster until they vanish (their color becomes darker and the slope reduces). Furthermore there are collisions, where a smaller, faster dune runs into a larger one. They merge and split again, forming two dunes of the same size as before, but in reverse order. This process was also described and modeled by Werner and Gillespie [20].

4.5 Parameter variations

4.5.1 Transport length

Increasing the transport length L while keeping the erosion rate unchanged means that the wind speed above the sand is increased, but the shear velocity is kept unchanged. To investigate how a change of wind velocity affects the outcome of the simulation a small area with a constant sand height of 0.75 was initialized.

As seen in Fig. 4.5 after a certain number of time steps barchans of the same magnitude are formed in the simulations with $L_{\min} \geq 2$. In the case where the effective transport length cannot grow larger than the cell size (Fig. 4.5(a)), it seems logical, that only noise is seen.

In Fig. 4.6 it can be seen, that a longer transport length per time step leads to a higher dune velocity. The relation between both variables is linear, which is expected.

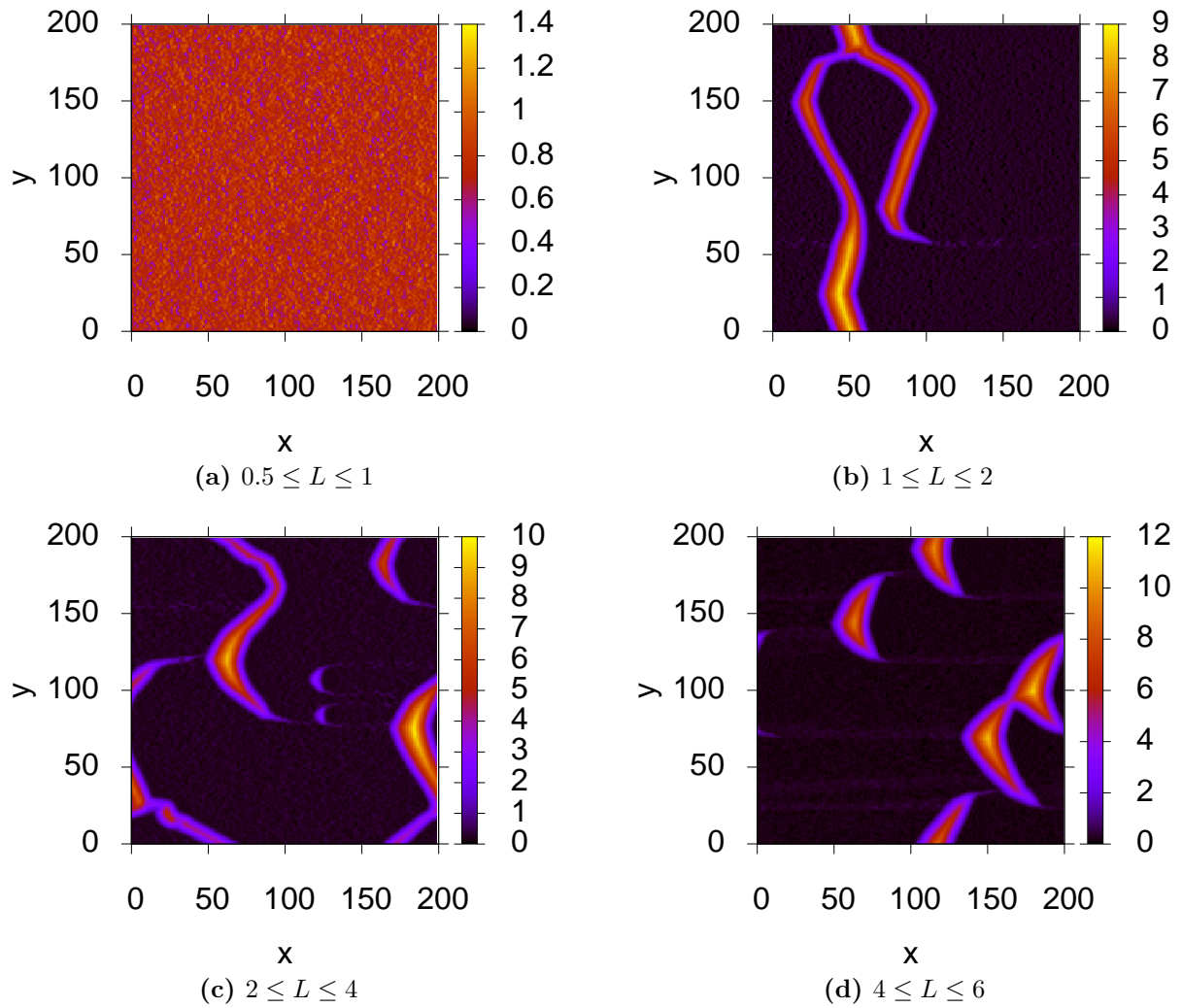
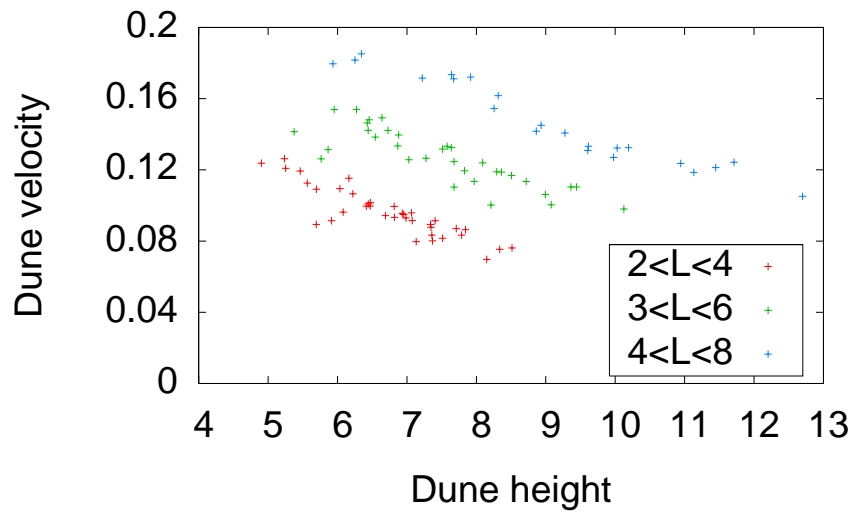
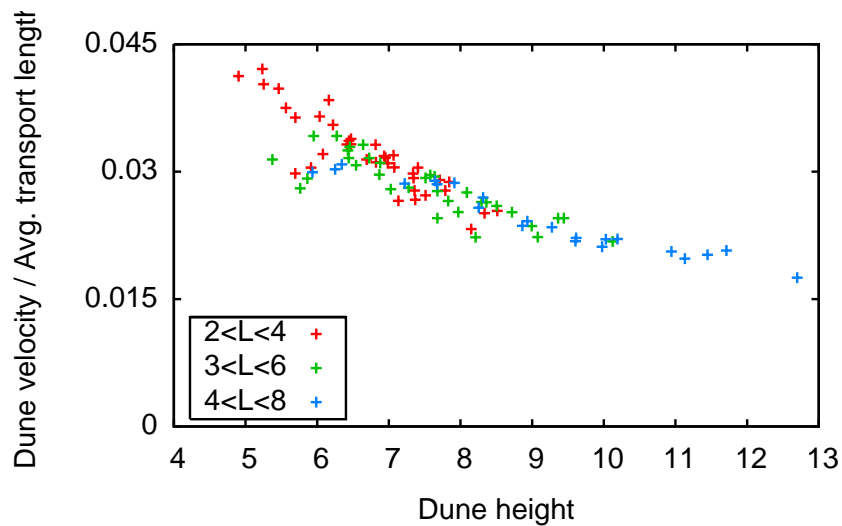


Fig. 4.5: Height map after simulating a long period of time. All parameters but the transport length were kept constant. The used cell size was $d = 1$.



(a) *not normalized*



(b) *normalized*

Fig. 4.6: *Dune velocities for different sized dunes. All parameters but the transport length were kept constant. Fig. (a) shows the functional relation between dune size and velocity, whereas in Fig. (b) the dune velocity is scaled down with the mean transport length per time step.*

4.5.2 Erosion rate

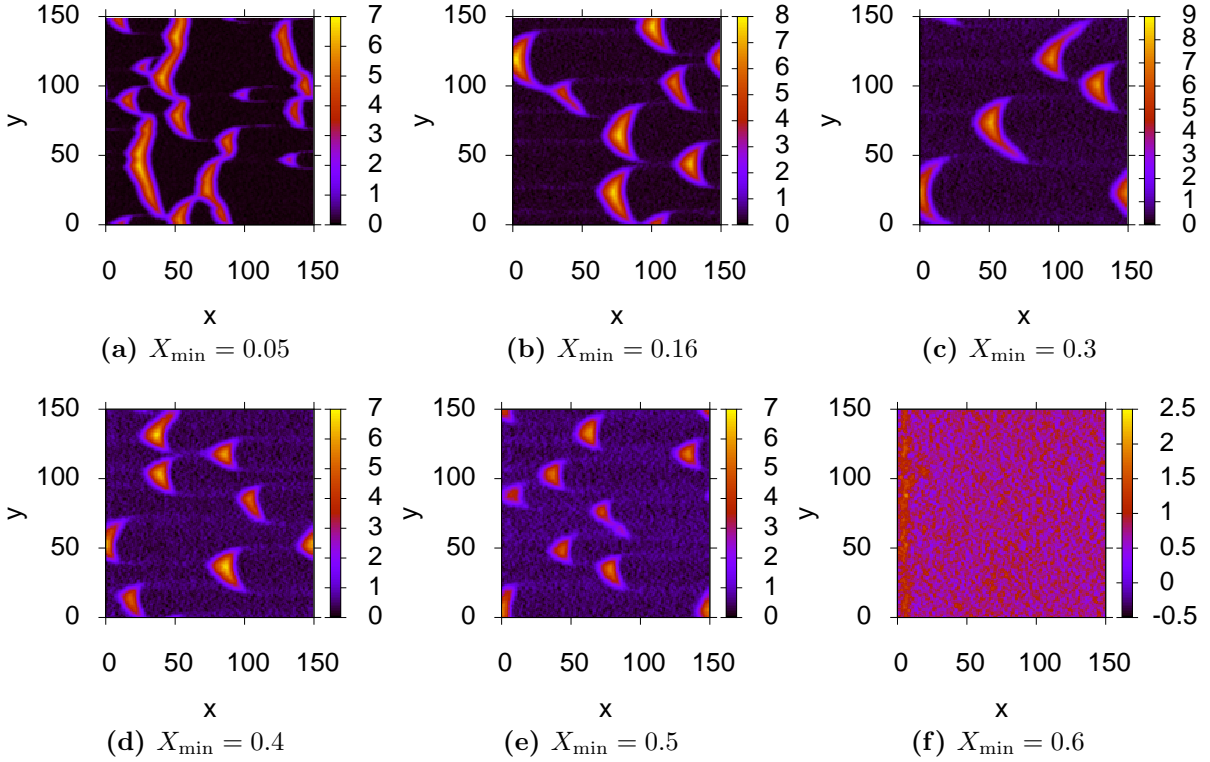


Fig. 4.7: Height maps after simulating a constant period of time with erosion rates varying within the range of 10 % from X_{\min} . All simulations were started with a flat sand sheet of height \bar{h} . The other parameters have been kept constant.

Increasing only the erosion rate means that more material is lifted into the air every time step without changing the transport distance. This corresponds to increasing the velocity gradient of the wind, while leaving the velocity in the height, where most of the sand is transported constant, which is (especially in the most common case of mixed grain sizes) impossible even in a wind tunnel.

In Fig. 4.7 it can be seen that stronger erosion leads to smaller dunes. A larger amount of eroded sand leads to more transported sand and therefore more sand is situated between the dunes instead of on the dunes at the same time. This effect can also be seen as bright spots between the dunes in the figure. Fig. 4.7(f) shows, that with a sufficiently strong erosion only noise is left. This is because no small scale structures can persist long enough to accumulate larger amounts of sand around them.

In Fig. 4.8 it becomes visible, that dunes move faster with a higher degree of erosion. This is also plausible since the amount of sand belonging to one dune can be carried away faster when more sand can be removed and transported in each time step. However a doubled erosion rate does lead to less than a doubled velocity, so there is no linear behavior like it was the case considering the transport length. An explanation could

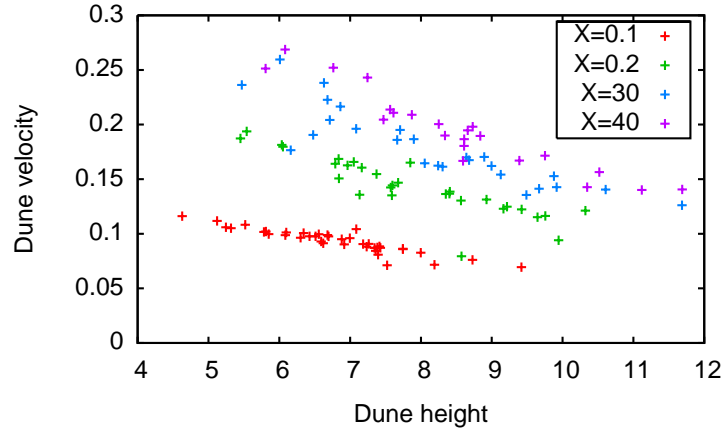


Fig. 4.8: *Dune velocities for dunes with different sizes. The only parameter changed is the erosion rate, which varied within the range of 10 % from X_{\min} .*

be, that with more sand sedimented on one cell and more sand transported, a greater portion of sand might get stuck along its way.

A result which can be seen from videos, but only be guessed from Fig. 4.7(a) is, that the time it takes until the dunes are shaped grows with less erosion applied, because it takes longer to carry the sand to another spot.

4.5.3 Total amount of sand

As discussed by Livingstone and Warren [13] approximately unidirectional wind leads to the formation of barchans as long as there is not much sand available. If there is a large amount of sand available, transverse dunes are formed.

Fig. 4.9 confirms this observation: As soon as the average sand height exceeds the amount of eroded sand per cell and time step, barchan dunes are formed (Fig. 4.9(b)). These cover a larger area and merge if the initial height is further increased (Figs 4.9(c)-(d)). When reaching $\bar{h} \approx 6$ all dunes are connected in several stripes transverse to the wind direction (Fig. 4.9(e)). In Fig. 4.9(f) it can be seen, that with a sufficient amount of sand the bottom becomes permanently covered with a sand sheet. This results in a dune height (over the average height or over the height of the valleys between dunes) being independent of the sand amount.

Fig. 4.10 shows, that the maximum height of a dune (spotted in a small simulated area) grows with the available amount of sand. The growth is biggest at very small amounts of sand. This is plausible, since the additional volume of material needed to enlarge any object by a certain scale grows with its length cubed. However this is only the case up to a certain size of transverse dunes. At some point ($\bar{h} \approx 12$ in the simulation shown here) the slopes of two neighboring dunes will meet and therefore no uncovered area between them is left. Further increasing the volume of sand available then only increases the total height at any place in the simulated area by an offset equal to the difference in average altitude. The height of the dunes relative to the height at the valleys between

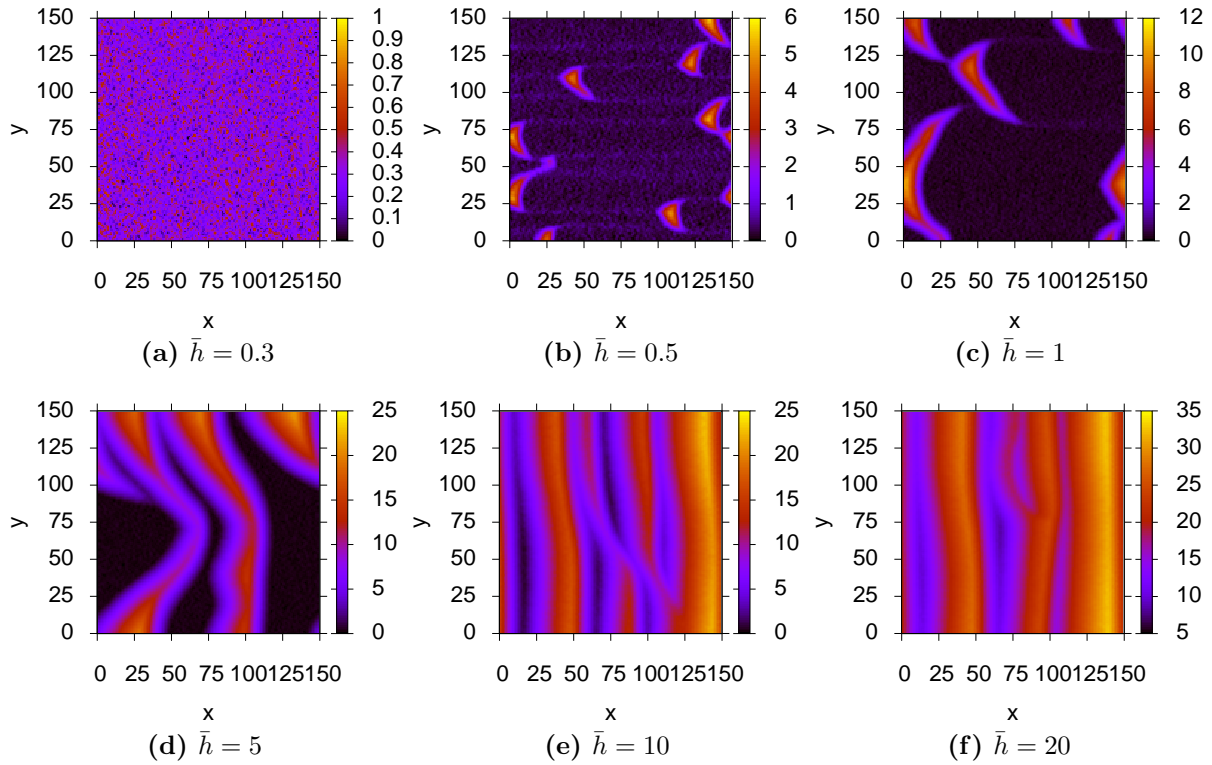


Fig. 4.9: Height maps after simulating a long period of time with a given constant initial height. All simulations were started with a flat sand sheet of height \bar{h} . The other parameters have been kept constant.

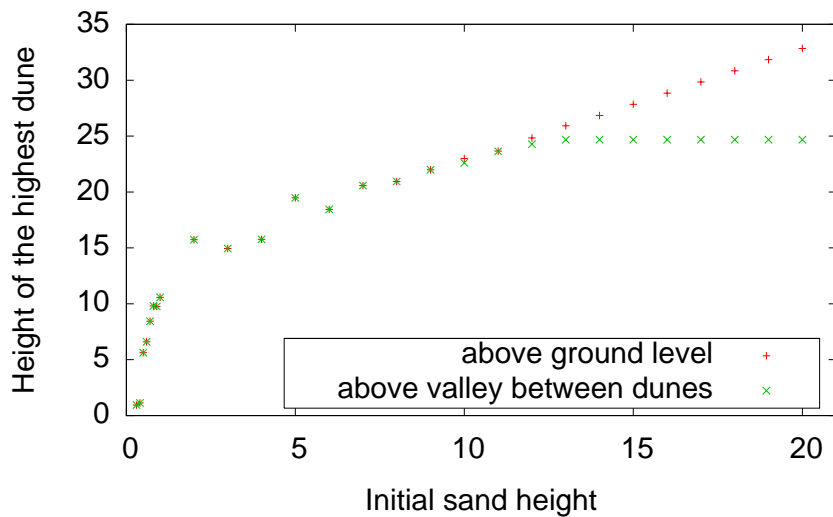


Fig. 4.10: This diagram shows the height of the highest dune found in the simulated area for simulations each started with a flat sand sheet of the height \bar{h} . All other parameters have been kept constant.

them remains unchanged.

4.6 Correlation of dune size and dune velocity

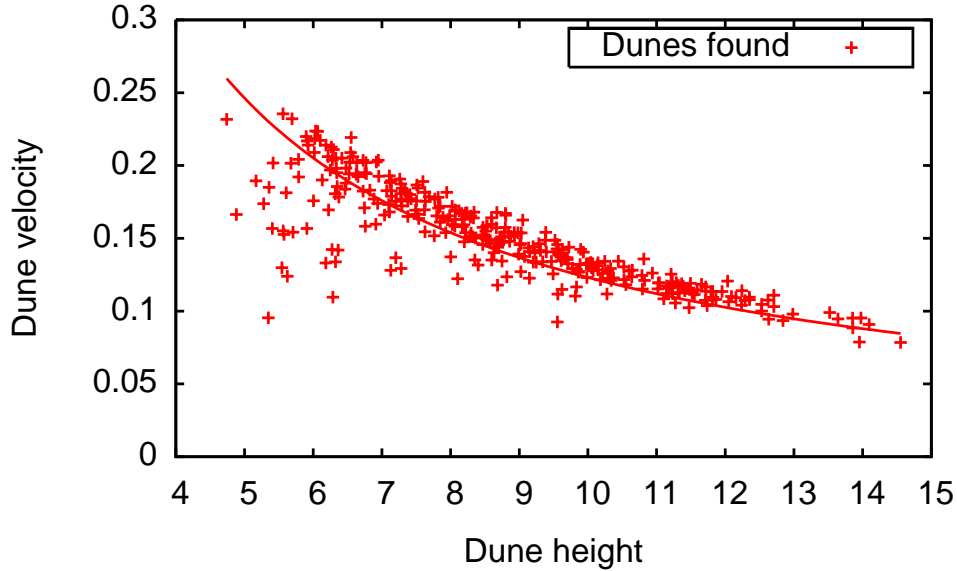


Fig. 4.11: *Dune velocities for dunes of different sizes with $3 \leq L \leq 6$*

To verify whether the dune velocity depends on the dune height in a hyperbolic manner as predicted in section 2.5, several runs were done with the same parameters ($3 \leq L \leq 6$), but with a differing sand supply (to achieve a larger range of dune heights) were performed. In Fig. 4.11 it can be seen, that such a correlation can be found in the model. Some of the data points lie significantly under the curve drawn in the figure, corresponding to dunes much slower than they should be. These are artifacts from the analysis. To determine the velocities single dunes were extracted from the t - x -diagrams as seen in Fig. 4.4. Then, the velocities were calculated from the slope. When a dune loses sand, it becomes faster, but since the slope is calculated from a longer range of time the velocity found might correspond to a dune height differing from the one that was determined at the end of the simulation (seen on the upper border of the diagram).

5 Conclusions and outlook

The goal of this thesis was to find a model that can simulate turbulences and structure creation in them. The complex process of dune creation could be simulated with a relatively simple set of abstract rules using a cellular automaton.

When simulating the creation of a sand pile, the end state looks promising, but no SOC-behavior could be found in the distribution of avalanche sizes. Another automaton for the sliding process was written. Its avalanche size distributions comply well with experimental data which also means, that SOC behavior was found (especially for very small sand piles). This model was however very slow and since for the simulation of dune fields the end state of a sliding process is much more important, than how it was achieved, this model was discarded.

Even with this deficit in one aspect of the problem good results could be found when simulating the formation and movement of dunes. It could be seen, that dunes keep their shape when moving, as long as they are sufficiently supplied with sand. Furthermore the observation, that much available sand leads to the formation of transverse dunes, while with less sand barchans will be created could be reproduced. Even the functional relation between dune velocity and dune height could be found in the results of the simulation.

This shows, that this fairly simple model can provide qualitative information about structure building and movement in wind blown sand. To receive quantitative information, it would be necessary to derive the absolute values of all used parameters from known parameters in the real world and even when this is accomplished, the used formulas might not approximate the processes well enough for quantitative data.

The next step to extend the model would be to introduce seasons with different wind speeds and directions. Furthermore it would be more realistic to have a real wind model from which the parameters for transport length and erosion are derived.

Acknowledgements

At the very end of this thesis I want to express my thanks to people, who helped me finishing this thesis. First of all I want to thank my supervisor Prof. Dr. Ralf Schneider.

Bibliography

- [1] G. Falkovich, A. Fouxon, and M. G. Stepanov, “Acceleration of rain initiation by cloud turbulence,” *Nature*, vol. 419, no. 6903, pp. 151–154, 2002.
- [2] N. Yoshioka, “A sandpile experiment and its implications for self-organized criticality and characteristic earthquake,” *Earth, planets and space*, vol. 55, no. 6, pp. 283–289, 2003.
- [3] K. Nagel and E. Raschke, “Self-organizing criticality in cloud formation?,” *Physica A: Statistical Mechanics and its Applications*, vol. 182, no. 4, pp. 519 – 531, 1992.
- [4] P. Bak and K. Sneppen, “Punctuated equilibrium and criticality in a simple model of evolution,” *Phys. Rev. Lett.*, vol. 71, pp. 4083–4086, Dec 1993.
- [5] S. Clar, B. Drossel, and F. Schwabl, “Forest fires and other examples of self-organized criticality,” *Journal of Physics: Condensed Matter*, vol. 8, no. 37, p. 6803, 1996.
- [6] R. O. Dendy and P. Helander, “Sandpiles, silos and tokamak phenomenology: a brief review,” *Plasma Physics and Controlled Fusion*, vol. 39, no. 12, p. 1947, 1997.
- [7] P. Bak, C. Tang, and K. Wiesenfeld, “Self-organized criticality: An explanation of the $1/f$ noise,” *Phys. Rev. Lett.*, vol. 59, pp. 381–384, Jul 1987.
- [8] P. Bak, C. Tang, and K. Wiesenfeld, “Self-organized criticality,” *Phys. Rev. A*, vol. 38, pp. 364–374, Jul 1988.
- [9] A. Mehta and G. C. Barker, “The dynamics of sand,” *Reports on Progress in Physics*, vol. 57, no. 4, p. 383, 1994.
- [10] R. A. Bagnold, *The physics of blown sand and desert dunes*. 1941.
- [11] J. J. Alonso and H. J. Herrmann, “Shape of the tail of a two-dimensional sandpile,” *Phys. Rev. Lett.*, vol. 76, pp. 4911–4914, Jun 1996.
- [12] S. R. Bishop, H. Momiji, R. Carretero-González, and A. Warren, “Modelling desert dune fields based on discrete dynamics,” *Discrete Dynamics in Nature and Society*, vol. 7, no. 1, pp. 7–17, 2002.
- [13] I. Livingstone and A. Warren, *Aeolian geomorphology: an introduction*. Addison Wesley, 1996.

- [14] D. M. Rubin and R. E. Hunter, “Bedform climbing in theory and nature,” *Sedimentology*, vol. 29, no. 1, pp. 121–138, 1982.
- [15] M. Gerhardt and H. Schuster, *Das digitale Universum. Zelluläre Automaten als Modelle der Natur*. Vieweg, 1995.
- [16] F. de Castro, “Computer simulation of the dynamics of a dune system,” *Ecological Modelling*, vol. 78, no. 3, pp. 205 – 217, 1995.
- [17] H. Nishimori and N. Ouchi, “Formation of ripple patterns and dunes by wind-blown sand,” *Phys. Rev. Lett.*, vol. 71, pp. 197–200, Jul 1993.
- [18] C. P. C. Prado and Z. Olami, “Inertia and break of self-organized criticality in sandpile cellular-automata models,” *Phys. Rev. A*, vol. 45, pp. 665–669, Jan 1992. Model for simulating avalanches. Only for large lattices.
- [19] G. A. Held, D. H. Solina, H. Solina, D. T. Keane, W. J. Haag, P. M. Horn, and G. Grinstein, “Experimental study of critical-mass fluctuations in an evolving sandpile,” *Phys. Rev. Lett.*, vol. 65, pp. 1120–1123, Aug 1990.
- [20] B. T. Werner and D. T. Gillespie, “Fundamentally discrete stochastic model for wind ripple dynamics,” *Phys. Rev. Lett.*, vol. 71, pp. 3230–3233, Nov 1993.
- [21] <http://gomyclass.com/wind.html>
Photo of the barchan dune [Online; accessed 08-July-2010].
- [22] http://ming.tv/flemming2.php/___show_article/_a000010-001929.htm
Photo of the cyclone [Online; accessed 08-July-2010].